Modeling the Melt Spinning of Polyethylene Terephthalate

Mariel L. Ottone and Julio A. Deiber

>> Version of Record - Apr 1, 2000

What is This?

Modeling the Melt Spinning of Polyethylene Terephthalate

MARIEL L. OTTONE AND JULIO A. DEIBER*
Instituto de Desarrollo Tecnológico
Para la Industria Química
Intec (UNL-Conicet)
Güemes 3450-(3000) Santa Fe, Argentina

ABSTRACT: A model is formulated to describe quantitatively the melt spinning of a polyethylene terephthalate (PET) within the low range of take up velocities. The rheology of the polymer melt is described with the Phan-Thien and Tanner constitutive equation for the stress tensor by considering both the instantaneous and retarded elastic responses. This rheological model gives appropriate predictions of the velocity and temperature profiles of the filament, within the framework of the spinning model proposed in this work. This conclusion arises when numerical results of this model are compared with experimental data as well as other calculations available in the literature.

KEY WORDS: melt fiber spinning, polyethylene terephthalate, melt rheology, retarded elastic response, melt heat transfer, elongational flow.

INTRODUCTION

IN FIBER MELT spinning, a bunch of polymer melt filaments are continuously drawn and simultaneously cooled with air in order to obtain solidified yarns which later compose the synthetic fiber in the bobbin (Figure 1 shows one filament only). Although melt spinning is a basic operation in the production of synthetic fibers, its fundamental model is still under intensive research, mainly because of the need of
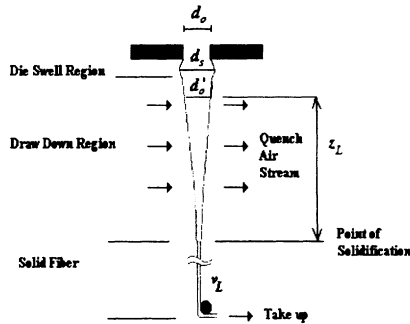
---

*Author to whom correspondence should be addressed.

FIGURE 1. Schematic of the melt spinning process involving one filament.

new knowledge concerning the non-isothermal response of viscoelastic materials. Several authors have proposed useful rheological models in order to study the non-isothermal process of the polyethylene terephthalate (PET) melt spinning [1–5]. Other works can be also found [3,6–8] where the melt spinning of this polymer is modeled as a Newtonian fluid, the viscosity of which depends upon temperature. From the modern literature, one may conclude that the thermo-rheological models proposed to predict the performance of the PET melt spinning at low processing velocities are still in progress for the usual take up velocity range (between 1000 to 3000 m/min) found in many industrial applications.

In this practical context, a model is formulated in this work to describe quantitatively the PET melt spinning at low take up velocities. Numerical results are compared with well documented experimental data of this process published previously by George [6]. The theoretical model follows the basic framework described by the pioneering work of Gagon and Denn [3] where, under the thin filament hypothesis [2,9] the balances of mass and momentum involving the inertial, gravitational and air-filament drag forces are solved numerically. These balance equations are also coupled to the average energy balance, which includes the mechanical dissipation term [5].

In our work, we use a better correlation for the heat transfer between air and filament which has been proposed recently by Denn [10]. In addition, the viscoelastic polymer is described through the linear superposition of two mechanical contributions. One of them considers the inelastic Newtonian response, in general attributable to the retardation effects of the macromolecular structure in the viscoelastic relaxation phenomena. This contribution to the total stress gives origin to the frequently designated "molecular" viscosity [11–14], and hence, to

the equivalent concept associated to the retarded elastic response of the whole model. The other contribution describes the instantaneous elastic response of the polymer in the sense discussed by Denn [15]. For this purpose, the Phan-Thien and Tanner rheological model is used here, where the thermal history is in addition considered through the term $d \ln T/dt$, which involves the rate of change of temperature (temperature T is expressed in °C throughout this work). This constitutive equation was also used by Gagon and Denn [3] and more recently by Devereux and Denn [5] by neglecting both effects in the rheological response of the PET; viz., the rate of change of temperature and the retarded elastic response.

We also carried out a rheometric study of this rheological model in order to evaluate the rheological parameters of the PET melt with experimental data reported by Gregory [16] involving the shear rate flow of a sample which had the same intrinsic viscosity as the PET used by George [6]. In fact, the sample under consideration here has an intrinsic viscosity $[\eta]_0 = 0.675$ dl/g and an average molecular weight $Mw = 43,744$ Da. This relevant experimental study available in the literature allowed us to find in a simple procedure, the shear stress τ as function of the shear rate D for this specified intrinsic viscosity at different temperatures, and mainly for that temperature at which George carried out his spinning experiments. In our thermo-rheological model, in addition, the relaxation time λ, the relaxation modulus G, and the thermophysical properties of the PET melt are considered functions of temperature, which also changes along the axial distance in the filament.

In order to have the same numerical reference point as that used by other authors, we also solve the non-isothermal spinning model of the PET by considering its melt as a Newtonian fluid with a viscosity that changes with temperature. Thus, pseudoplastic as well as viscoelastic effects are ignored in this part. These results are helpful to validate the numerical algorithm used by direct comparison with previous result published in the literature [3].

RHEOLOGICAL MODEL FOR THE PET MELT

The Phan-Thien and Tanner model for the stress tensor $\underline{\underline{\tau}}_p$ is used, which is the polymer contribution to the total stress $\underline{\underline{\tau}} = \underline{\underline{\tau}}_p + \underline{\underline{\tau}}_s$. Here, $\underline{\underline{\tau}}_s = 2\eta_s \underline{\underline{D}}$ is the Newtonian part of $\underline{\underline{\tau}}$ with viscosity η_s as discussed above. The counterpart concept of instantaneous elastic response is

obtained when η_s = 0 [15], as it is described later. Also, $\underline{\underline{D}} = (\underline{\nabla}\underline{v} + \underline{\nabla}\underline{v}^T)/2$ is the rate of deformation tensor and $\underline{v}$ is the axial velocity. Then for a melt density ρ that is weakly dependent on temperature, we can express,

$$\underset{=p}{\tau} + \lambda \frac{\delta}{\delta t} \underset{=p}{\tau} = 2\lambda G\underline{\underline{D}} \tag{1}$$

where the relaxation time λ depends on both thermal and mechanical histories as follows:

$$\lambda = \lambda_0(T) \exp[-\xi(tr\underset{=}{\tau})/G] \tag{2}$$

In Equation (2), $G = G_0(T\rho/T_r\rho_r)$ is the relaxation modulus that depends on temperature, and T_r = 295°C is the reference temperature used in this work. Also, ρ_r is the polymer density evaluated at T_r. Additionally tr indicates the trace of a tensor.

In Equation (1), the Gordon-Schowalter non-affine convective time derivative is applied and expressed,

$$\frac{\delta}{\delta t}\underset{=p}{\tau} = \frac{D}{Dt}\underset{=p}{\tau} - \underline{\underline{L}} \cdot \underset{=p}{\tau} - \underset{=p}{\tau} \cdot \underline{\underline{L}}^T - \underset{=p}{\tau} \frac{d\ln T}{dt} \tag{3}$$

where D/Dt is the time material derivative. Also, $\underline{\underline{L}} = \underline{\nabla}\underline{v} - \chi\underline{\underline{D}}$ with the constraint that $0 \leq \chi \leq 1$. In Equation (3), $d \ln T/dt$ arises from the consideration that the spring force associated to the end-to-end distance of a molecular strand in the polymer network has a temperature dependent rigidity [4]. It is also required that $\eta_s = \eta_p(1 - \alpha)/\alpha$ and $\eta_p = \lambda G$, so that for $\alpha = 1$ the instantaneous elastic response of the melt is obtained as it is described elsewhere [15,17].

In order to determine the rheological parameters of the above model for the PET melt with an intrinsic viscosity $[\eta]_0$ = 0.675 dl/g and an average molecular weight Mw = 43,744 Da, rheometric data for shear flow at different temperatures reported by Gregory [16] are used, who also found that

$$\lambda_0 = \lambda_{00} \exp\left[-11.9755 + \frac{6802.1}{(T + 273)}\right] \tag{4}$$

Therefore, from Equation (4), the thermal shift factor a_T is defined as

$$a_T = \frac{\lambda_0(T)}{\lambda_0(T_r)} = \frac{\lambda_0(T)}{\lambda_{00}(T_r)} = \exp\left[-11.9755 + \frac{6802.1}{(T + 273)}\right] \tag{5}$$
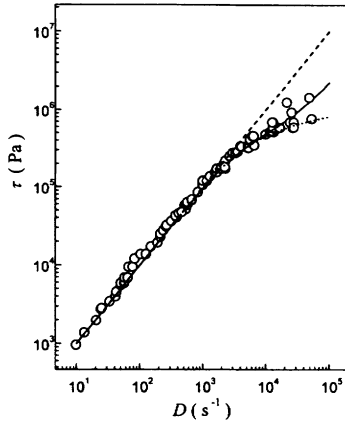
FIGURE 2. Shear stress as function of shear rate for a PET with an intrinsic viscosity $[\eta]_0$ = 0.675 dl/g and an average molecular weight Mw = 43,744 Da. Open circles are experimental data [16]. The solid line is the best fit with the Phan-Thien and Tanner model with retarded elastic response [Equations (6) to (11)] for $\alpha = 0.8$, $\chi = 4 \ 10^{-5}$, $\lambda_{00} = 0.016$ s, G_0 = 5245.9 Pa and $\xi = 9.25 \ 10^{-5}$. The dotted line refers to the prediction of the Phan-Thien and Tanner model with instantaneous elastic response for $\alpha = 1$, $\chi = 0$, $\lambda_{00} = 0.01425$ s, G_0 = 7017.5 Pa and $\xi = 9.25 \ 10^{-5}$. The best fitting of the Maxwellian fluid ($\alpha = 1$, $\chi = 0$, λ_{00} = 0.01425 s, $G_0 = 7017.5$ and $\xi = 0$) is indicated with a dashed line. The reference temperature is $T_r = 295°C$.

With Equation (5) and the molecular shift factor $B = 13.055$ of the reference (see Figure 7 of Gregory's work [16]) experimental data of shear stress τ as function of shear rate D can be readily obtained as it is shown in Figure 2.

In order to obtain the best fit of these experimental data with the rheological model, one has to specialize Equations (1) to (4) for a shear flow field. With the purpose of simplifying the nomenclature of this work, these equations are written in the cylindrical coordinate system, which is also used later in the melt spinning model. Thus,

$$\frac{\partial}{\partial t} \tau_p^{zz} = -\frac{K}{\lambda_0} \tau_p^{zz} + \tau_p^{rz}\left(1 - \frac{\chi}{2}\right)D + \tau_p^{zr}\left(1 - \frac{\chi}{2}\right)D \tag{6}$$

$$\frac{\partial}{\partial t} \tau_p^{rr} = -\frac{K}{\lambda_0} \tau_p^{rr} - \tau_p^{rz}\frac{\chi}{2}D - \tau_p^{zr}\frac{\chi}{2}D \tag{7}$$

$$\frac{\partial}{\partial t} \tau_p^{zr} = -\frac{K}{\lambda_0} \tau_p^{zr} + \tau_p^{rr}\left(1 - \frac{\chi}{2}\right)D - \tau_p^{zz}\frac{\chi}{2}D + GD \tag{8}$$

$$\frac{\partial}{\partial t} \tau_p^{\theta\theta} = -\frac{K}{\lambda_0} \tau_p^{\theta\theta} \tag{9}$$

$$K = \exp\left[\frac{\xi}{G}(\tau_p^{zz} + \tau_p^{rr} + \tau_p^{\theta\theta})\right] \tag{10}$$

where,

$$\underline{\underline{D}} = \left\{\begin{matrix} 0 & \frac{1}{2}D & 0 \\ \frac{1}{2}D & 0 & 0 \\ 0 & 0 & 0 \end{matrix}\right\} \tag{11}$$

and $D = (dv/dr)$. In addition, $\tau_s^{zz} = \tau_s^{rr} = \tau_s^{\theta\theta} = 0$ and $\tau_s^{zr} = \eta_s D$.

Unfortunately, the steady stresses cannot be obtained explicitly from the above equations. Therefore, a simple way to find the shear stress $\tau = \tau^{zr} = \tau_p^{zr} + \tau_s^{zr}$ is to solve these equations numerically from the inception of the shear flow until the asymptotic steady state is reached. In order to calculate this steady state, we write the time derivatives in Equations (6) to (9) in discrete form (forward finite differences) and apply the fourth order Runge-Kutta algorithm. The time step used is 10^{-4} s and the steady stresses are found for $\left|(\tau_{\underline{\underline{p}}}^{i+1} - \tau_{\underline{\underline{p}}}^{i})/\tau_{\underline{\underline{p}}}^{i}\right| \leq 10^{-6}$ where superscript i indicates the number of time steps being carried out. Thus, after satisfying this criterion, the total shear stress τ as function of shear rate D can be readily calculated. This result is presented in Figure 2 with a solid line for $\alpha = 0.8$ which belongs to the case of retarded elastic response. The other rheological parameters obtained in the best fit of experimental data are indicated in the figure caption. Also in Figure 2, the dotted line refers to the rheological model prediction with instantaneous elastic response for $\alpha = 1$ and $\chi = 0$. In this figure, the best fit of the Maxwellian fluid, which gives the same response as the Newtonian fluid in shear rate, is presented with a dashed line. Additionally, since the rheological characterization of the PET melt with the above model requires the evaluation of five parameters (χ, ξ, λ_{00}, α and G_0) it is clear that one must also carry out, apart from the best fit of the shear stress–shear rate data, a finer adjustment of these parameters simultaneously with the performance of the spinning model presented in the next section. In the same context of rheological characterization, more recently Hatzikiriakos et al. [18] evaluated the rheological parameters of three types of PET through dynamic and capillary rheometries. Unfortunately, these polymers were of different average molecular weights

from that used by George [6], as we inferred from the zero shear rate viscosity values reported by these authors.

For the purpose of visualizing the behavior of the PET melt under rheometric elongational flow once it has been characterized through the shear rate rheometry, we solved Equations (1) to (4) for,

$$\underline{\underline{D}} = \left\{ \begin{matrix} \dot{\varepsilon} & 0 & 0 \\ 0 & -\dfrac{1}{2}\dot{\varepsilon} & 0 \\ 0 & 0 & -\dfrac{1}{2}\dot{\varepsilon} \end{matrix} \right\} \tag{12}$$

where $\dot{\varepsilon}$ is the elongational rate. In a similar situation as the one described above for the shear rate rheometry, the steady stresses cannot be obtained explicitly in elongational flow from the rheological model and the kinematics expressed by Equation (12). Therefore, the elongational viscosity $\eta_e = (\tau^{zz} - \tau^{rr})/(3\eta_0\dot{\varepsilon})$, where $\eta_0 = \eta_p + \eta_s$, is found here by solving numerically the following equations for the inception of the elongational flow until the asymptotic steady state is reached:

$$\frac{\partial}{\partial t}\,\tau_p^{zz} = -\frac{K}{\lambda_0}\,\tau_p^{zz} + 2\tau_p^{zz}(1-\chi)\dot{\varepsilon} + 2G\dot{\varepsilon} \tag{13}$$

$$\frac{\partial}{\partial t}\,\tau_p^{rr} = -\frac{K}{\lambda_0}\,\tau_p^{rr} - \tau_p^{rr}(1-\chi)\dot{\varepsilon} - G\dot{\varepsilon} \tag{14}$$

$$\frac{\partial}{\partial t}\,\tau_p^{\theta\theta} = -\frac{K}{\lambda_0}\,\tau_p^{\theta\theta} - \tau_p^{\theta\theta}(1-\chi)\dot{\varepsilon} - G\dot{\varepsilon} \tag{15}$$

where,

$$K = \exp\left[\frac{\xi}{G}(\tau_p^{zz} + 2\tau_p^{rr})\right] \tag{16}$$

Once more, in order to find the steady stresses, we write in discrete form the time derivatives in Equations (13) to (15) and apply the same numerical procedure as that used for the shear flow analyzed above. Thus, after satisfying the converge criterion, $(\tau^{zz} - \tau^{rr})$ can be readily calculated as function of the elongational rate $\dot{\varepsilon}$. The steady elongational viscosity η_e is presented in Figure 3 for the cases of instantaneous ($\alpha = 1$) and retarded ($\alpha = 0.8$) elastic responses. Also the
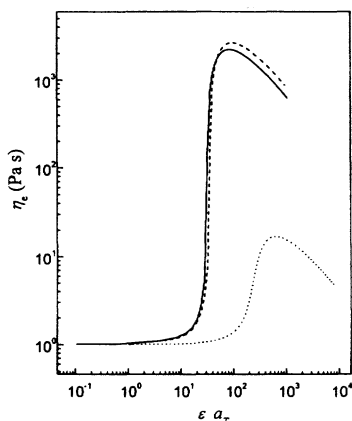
FIGURE 3. Elongational viscosity as function of elongational rate for the PET with an intrinsic viscosity $[\eta]_0 = 0.675$ dl/g and an average molecular weight $Mw = 43,744$ Da. The solid line is obtained by using the Phan-Thien and Tanner model with retarded elastic response for $\alpha = 0.8$. The dashed line refers to the prediction of the Phan-Thien and Tanner model with instantaneous elastic response for $\alpha = 1$. The reference temperature is $T_r = 295°C$. The response of the one mode Phan-Thien and Tanner model used in Reference [3] is indicated with a dotted line.

elongational viscosity of the one mode Phan-Thien and Tanner model used in Reference [3] is reported in this figure. Thus, one finds that the differences in rheological parameters causes a significant change in the elongational response of the rheological model.

MELT SPINNING MODEL

In the basic process of melt spinning, the polymer melt is sent to a bunch of fine capillary tubes by a gear pump at a well specified flow rate Q_0 and temperature T_0. At the exits of these extrusion capillaries of diameter d_0, the filaments are quenched with cold air. As a consequence of this cooling, the polymer gets the glassy temperature T_g at a given axial distance (Figure 1). Under this condition, a roll with a tangential velocity v_L, designated also the take up velocity, is able to receive the solid fiber which can be then subjected to further mechanical and thermal treatments, depending this decision on the final use given to the fiber in the textile industry. In our model $v'_0 = v_0(d_0/d'_0)^2$ is the initial average velocity of the filament at $z = 0$ (the position $z = 0$ with filament diameter d'_0 is defined later and it depends on the consideration of either the instantaneous or the retarded elastic responses).

Also, $v_0 = Q_0/\pi d_0^2$ is the average velocity of the polymer melt in the capillary. In the specific case of the PET melt, for draw ratios $DR = v_L/v_0' < 220$, the fiber formed does not present a crystalline phase [19]. Therefore, one should expect only the partial ordering of the polymer amorphous phase for the cases studied in our work, where the maximum draw ratio analyzed is $DR = 165$. This specific aspect is taken into account in the model proposed next.

A macroscopic mass balance in the filament is formulated by equating the mass flow rate through the capillary to that at any filament axial position z,

$$\rho_0 Q_0 = \rho \frac{\pi d^2}{4} v \tag{17}$$

where $\rho = (1356 - 0.5T)$ kg/m^3 [20] is the PET melt density that varies with temperature T evaluated at the axial position z. Thus, the product $\rho_0 Q_0$ defines the mass flow rate in the capillary at temperature T_0. In Equation (17), the filament diameter d is a function of axial position z.

The momentum balance of the filament is obtained by neglecting the effect of surface tension [3]. Thus,

$$\frac{\partial}{\partial z}\left[\frac{\pi d^2}{4}(\tau^{zz} - \tau^{rr})\right] = \frac{\pi d}{2}\rho_a v^2 C_f + \rho\left[Q\frac{\partial v}{\partial z} - \frac{\pi d^2 g}{4}\right] \tag{18}$$

where τ^{zz} and τ^{rr} are the axial and radial components of the total stress tensor $\bar{\bar{\tau}}$.

In Equation (18), ρ_a denotes the density of air, and g is the acceleration due to gravity. Also C_f is the air drag coefficient, which varies with axial position. In order to evaluate C_f the correlation proposed by Denn [10] is used,

$$C_f = 2\,\beta\left(\frac{\eta_a}{\rho_a v d}\right)^{0.61} \tag{19}$$

where η_a is the viscosity of air. In this work, $\beta = 0.4$ and 0.44 are used for the retarded and instantaneous elastic responses, respectively. These values are within the admissible range $0.37 \leq \beta \leq 0.6$ reported in the literature [20], and also give the best prediction of the model in relation to experimental data.

The balance of energy with negligible axial conduction is [5],

$$\rho c_v v \frac{\partial T}{\partial z} = -\frac{4h}{d}(T - T_a) + (\tau^{zz} - \tau^{rr})\frac{\partial v}{\partial z} \tag{20}$$

where $c_v = (1256.1 + 2.51T)$ J/kg °C [20] is the heat capacity of the filament, and T and T_a are the filament and air temperatures, respectively. The heat transfer coefficient h, which varies with axial position, is expressed through the combination in series of the external h_e and internal h_i heat transfer coefficients; thus,

$$h = \frac{1}{(1/h_e + 1/h_i)} \tag{21}$$

The correlation published by Denn [10] is used in this work in order to evaluate h_e associated to the heat transfer by convection of the cooling air. Therefore,

$$\frac{h_e d}{k_a} = \beta \, \mathrm{Pr}^{1/3} \, \mathrm{Re}^{0.39} \left[1 + 64 \left(\frac{v_a}{v} \right)^2 \right]^{0.166} \tag{22}$$

where v_a is the air cross-flow velocity, and k_a is the thermal conductivity of air. The Prandtl number $\mathrm{Pr} = \eta_a c_{pa}/k_a$ is around 0.684 for air at $T_a = 30$°C. The heat transfer coefficient h_i is estimated from the following scaling relationship of pure heat conduction in the fiber,

$$h_i = \frac{2k_s}{d\psi} \tag{23}$$

where $0 < \psi < 1$ is a lumped parameter to be determined with the best numerical prediction of the filament temperature profile in relation to the available experimental data. In this work, $\psi = 0.22$ and 0.26 were the best values for the retarded and instantaneous elastic responses, respectively. In Equation (23), $k_s = 0.037$ W/m °C is the thermal conductivity of the PET melt considered to be a constant.

From Equations (17) to (23), it is clear that the steady axial profiles of both cross sectional averaged velocity v and temperature T in the polymer are studied by considering the thin filament hypothesis described in the literature [2]. This hypothesis is based on the fact that the filament diameter is very smooth along the spinneret after the swelling formation zone. Thus, Keunings et al. [9] found numerically that this hypothesis is valid downstream from the point of maximum extrudate swell where the diameter is d_s (Figure 1). We will show then that for the Phan-Thien and Tanner model with retarded elastic response, this initial condition can be put at the maximum extrudate swell by considering $d'_0 = d_s$. In addition, in our calculations an initial cross section 100% greater than that of the capillary cross section is considered by following the proposal of George [6] for this problem.

NUMERICAL SOLUTION OF THE SPINNING MODEL

With the equation of continuity and assuming that density changes with temperature are small, one readily shows that the kinematics in the spinning filament satisfy the following rate of deformtion tensor [1,2],

$$
\underline{\underline{D}} = \left\{ \begin{matrix} \dfrac{\partial v}{\partial z} & 0 & 0 \\[2ex] 0 & -\dfrac{1}{2}\dfrac{\partial v}{\partial z} & 0 \\[2ex] 0 & 0 & -\dfrac{1}{2}\dfrac{\partial v}{\partial z} \end{matrix} \right\} \tag{24}
$$

Therefore, from Equations (1), (3), (18), (20) and (24) we obtain after considerable algebra,

$$
\left\{ \begin{matrix} \dfrac{\partial v}{\partial z} \\[2ex] \dfrac{\partial f}{\partial z} \\[2ex] \dfrac{\partial}{\partial z}\tau_p^{zz} \\[2ex] \dfrac{\partial}{\partial z}\tau_p^{rr} \\[2ex] \dfrac{\partial T}{\partial z} \end{matrix} \right\} = \left\{ \begin{matrix} 1 & 0 & 0 & 0 & 0 \\[1.5ex] 0 & -\dfrac{3}{\rho v}\eta_s & -\dfrac{1}{\rho v} & \dfrac{1}{\rho v} & -\dfrac{3f}{\rho v}\dfrac{d\eta_s}{dT} \\[2ex] 0 & 0 & 1 & 0 & -\dfrac{1}{T}\tau_p^{zz} \\[2ex] 0 & 0 & 0 & 1 & -\dfrac{1}{T}\tau_p^{rr} \\[2ex] 0 & 0 & 0 & 0 & 1 \end{matrix} \right\}^{-1} \left\{ \begin{matrix} C_1 \\ C_2 \\ C_3 \\ C_4 \\ C_5 \end{matrix} \right\} \tag{25}
$$

where,

$$
\left\{ \begin{matrix} C_1 \\ C_2 \\ C_3 \\ C_4 \\ C_5 \end{matrix} \right\} = \left\{ \begin{matrix} f \\[2ex] \dfrac{g}{v} - \dfrac{v^{1.5}\rho_a C_f}{\rho\left(\dfrac{Q}{\pi}\right)^{0.5}} - \left[1 + (\tau_p^{zz} + 2\eta_s f - \tau_p^{rr} + \eta_s f)\dfrac{1}{\rho v^2}\right]f \\[3ex] \dfrac{\tau_p^{zz}}{v}\left(-\dfrac{K}{\lambda_0} + 2f(1-\chi)\right) + \dfrac{2G}{v}f \\[3ex] \dfrac{\tau_p^{rr}}{v}\left(-\dfrac{K}{\lambda_0} - f(1-\chi)\right) - \dfrac{G}{v}f \\[3ex] -\dfrac{4h}{\rho c_v d v}(T - T_a) + \dfrac{f}{\rho c_v v}(\tau_p^{zz} + 2f\eta_s - \tau_p^{rr} + f\eta_s) \end{matrix} \right\} \tag{26}
$$

and $f = (dv/dz)$.

The above non-linear system of first order differential equations expressed as $\dot{x} = A^{-1}(x) \cdot b$ [21] can be solved with the appropriate initial conditions for velocity, temperature and stresses. Nevertheless, in practice one may know the value of the axial velocity at the initial position calculated from $v_0' = v_0(d_0/d_0')^2$ (Figure 1) as well as the melt temperature at the extrusion capillary only. Unfortunately, the initial stresses are not known beforehand and they must be found through a numerical iterative process already described in the literature [2,3,21]. For this purpose there are available two additional data at the point where the polymer reaches the glassy temperature T_g. Thus at the distance z_L (Figure 1) one knows the take up velocity $v_L = DRv_0'$, and also the value of the glassy temperature, which for the case of the PET studied here is $T_g = 70°C$. These boundary conditions introduce an abrupt change in the numerical velocity profile (see Figure 4) because at $z = z_L$ the glass transition of the polymer is reached and v becomes definitely constant.

The iterative process consists of initializing the viscoelastic tensions τ_p^{zz} and τ_p^{rr} at $z = 0$ (this position is placed at the maximum swelling of the filament for the case of retarded elastic response; viz., $d_0' = d_s$) and solving the system of equations described above iteratively with the fourth order Runge-Kutta method, until one reproduces the value assigned to T_g and v_L at a calculated z_L, with the following convergence criteria:

$$|v^k - v_L|/|v_L| \leq E_v$$

$$|T^k - T_g|/|T_g| \leq E_T$$

where k indicates the number of axial step size used to reach z_L and E_v and E_T are the relative convergence errors associated to velocity and temperature profiles, respectively.

In addition, it is known that only one stress, say $\tau_p^{zz}(0)$, at the initial condition shall be iterated while the other is fixed with a constant ratio $Rel = \tau_p^{rr}/\tau_p^{zz}$ at $z = 0$. Thus, for an inelastic fluid this ratio is exactly $-1/2$ and for a viscoelastic melt $-1/2 \leq Rel \leq 0$ [22,23]. Since in our model we consider, in addition to previous works, the constitutive equation of Phan-Thien and Tanner with retarded elastic response, the initial value $f = 0$ is also required in Equation (26), which is the best estimate for the velocity derivative at the maximum extrudate swell. In fact, we found that for $f \to 0$, numerical solutions of v and T do not depend on the value assigned to this derivative.
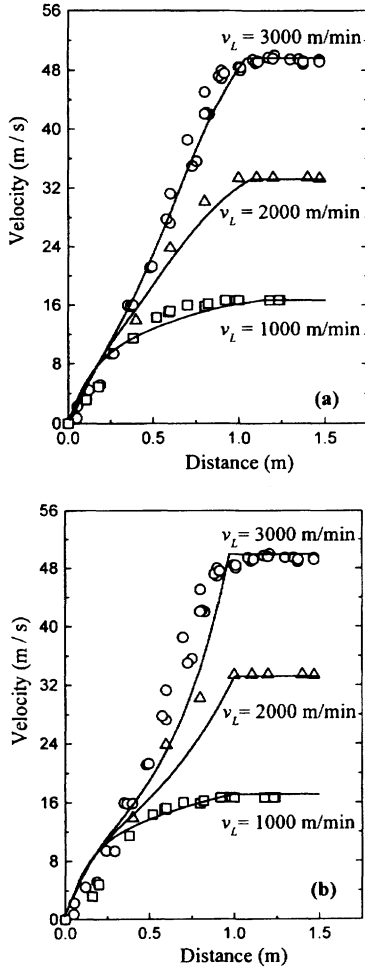
FIGURE 4. Numerical predictions (solid lines) of the filament axial velocity profile with the Phan-Thien and Tanner model for the spinning conditions of Table 1. Velocity experimental data [6] are reported with symbols: (a) retarded elastic response for $\alpha = 0.8$, $\beta = 0.4$ and $\psi = 0.22$; (b) instantaneous elastic response for $\alpha = 1$, $\beta = 0.44$ and $\psi = 0.26$.

On the other hand, when the rheological model with instantaneous elastic response is used ($\alpha = 1$) the condition $f = 0$ is not required anymore and the position $z = 0$ is not well determined in relation to the capillary exit. Usually, authors suggest to put it around two to four capillary diameters below the capillary exit [9]. Therefore, we study this case numerically to visualize the effect of choosing the point $z = 0$ at different positions considering that they must be physically placed after the maximum swelling diameter. In this sense, it was found numerically that for the experimental results analyzed in this work, the relation $d_0' = 1.44d_0$ is appropriate with the additional constraint that $\partial v/\partial z > 0$ at $z = 0$ (this value of d_0' corresponds to an initial cross-sectional area that is 100% greater than that of the capillary cross-sectional area as it was proposed previously [6]). These results clearly indicate that d_0' does not belong to the maximum swell diameter for the instantaneous elastic response of the rheological model.

In the numerical program, it is considered that the filament continues the cooling down process after the position z_L at the constant velocity v_L without any further stretching. Therefore, an analysis of convergence of the numerical algorithm described above is carried out. For this purpose, the Phan-Thien and Tanner model with retarded elastic response and the parameters evaluated in the previous section were used for the spinning conditions reported by George [6] (see Table 1) when the take up velocity was $v_L = 3000$ m/min ($DR = 165$). It was found that the results obtained were enough invariant for: $10^{-3} \leq \Delta\tau_p^{zz}(0) \leq 10^{-1}$ Pa, $10^{-5} \leq \Delta z \leq 10^{-3}$ m and $-1/2 \leq Rel \leq 0$.

In particular, we studied the effect of $\Delta\tau_p^{zz}(0)$ on the numerical results obtained when the convergence criteria were equal and fixed at $E = E_v = E_T = 10^{-4}$, and the axial step size was $\Delta z = 10^{-5}$ m. It was thus found that for $\Delta\tau_p^{zz}(0) \leq 0.5$ Pa the values of z_L, $v_L = DRv_0'$ and T_g were invariant in the six digits after the decimal point. The next step

Table 1. Conditions for the spinning experiments of George [6].

Intrinsic viscosity, $[\eta]_0$ dl/g	0.675
Extrusion temperature, T_0°C	300
Air temperature, T_a°C	30
Air velocity, v_a m/s	0.2
Capillary diameter, d_0 m	0.25×10^{-3}
Initial diameter, d_0' m	0.36×10^{-3}
Initial velocity, v_0' m/s	0.303

Table 2. Effect of the convergence criterion
$E = E_v = E_T$ on relevant numerical results
for $\Delta\tau_p^{zz}(0) = 0.1$ Pa, and $\Delta z = 10^{-5}$ m.

E	$\tau_p^{zz}(0)$ Pa	z_L m	v_L m/s	T_g °C
10^{-2}	5.25900 10^3	1.0411099	50.0006	69.9991
10^{-3}	5.25905 10^3	1.0411099	49.9997	69.9992
10^{-4}	5.25910 10^3	1.0411099	49.9988	69.9993
10^{-5}	5.25930 10^3	1.0411099	49.9954	69.9997

was to study the effect of the convergence criterion E, for $\Delta\tau_p^{zz}(0) = 0.1$ Pa, and $\Delta z = 10^{-5}$ m. Table 2 shows the most relevant results thus obtained and indicates that for $E \leq 10^{-4}$ quite precise results can be obtained for practical situations. In this context of analysis, the effect of the step size Δz on numerical results was also required. With this purpose, we fixed $E = 10^{-5}$ and $\Delta\tau_p^{zz}(0) = 0.1$ Pa and varied the step size as it is shown in Table 3. It was readily found that $\Delta z < 10^{-4}$ m is small enough for the accuracy of the results.

RESULTS AND DISCUSSION

Figures 4(a) and (b) show the axial velocity profiles obtained numerically with Equations (25) and (26) and the Phan-Thien and Tanner rheological model for the cases of retarded ($\alpha = 0.8$) and instantaneous ($\alpha = 1$) elastic responses under spinning flow. In this figure, numerical results are compared with experimental data [6] for a PET melt with an intrinsic viscosity of 0.675 dl/g. Figure 4(a) shows that the rheological model with retarded elastic response can predict quite well the spinning of the PET melt for the three take up velocities studied here. These predictions are better than those obtained with the rheological

Table 3. Effect of the axial step size Δz on
relevant numerical results for
$E = 10^{-5}$ and $\Delta\tau_p^{zz}(0) = 0.1$.

Δz m	$\tau_p^{zz}(0)$ Pa	z_L m	v_L m/s	T_g °C
10^{-3}	5.4691 10^3	1.0429999	49.9947	69.9598
10^{-4}	5.2784 10^3	1.0412999	49.9949	69.9943
10^{-5}	5.2593 10^3	1.0411099	49.9954	69.9997

model that involves the instantaneous elastic response [Figure 4(b)].
This conclusion is discussed quantitatively in the next paragraph. In
both cases, however, the parameters ξ and χ that affect the non-linear
terms of the rheological model are rather small indicating that the
PET melt has a viscoelastic response similar to that of the Maxwell
fluid under the spinning flow conditions. This is not true, however, for
shear flow (see also Figure 2).

In order to analyze the quality and goodness of the model predic-
tions, relative percentile differences D_v and D_T between numerical and
experimental values are defined for both velocity and temperature ax-
ial profiles. These definitions are

$$D_v = \sum_{i=1}^{N} \left| \frac{(v_{num}^i - v_{exp}^i)}{v_{num}^i} \right| \frac{100}{N} \quad \text{and} \quad D_T = \sum_{i=1}^{N} \left| \frac{(T_{num}^i - T_{exp}^i)}{T_{num}^i} \right| \frac{100}{N}$$

where N is the number of experimental points of each variable avail-
able for the three take up velocities. For the case analyzed in Figure
4(a), D_v does not exceed 4.5% (Table 4). When the instantaneous elas-
tic response is considered [Figure 4(b)], however, D_v is between 4.1 and
6.7% as reported in Table 4, indicating that the rheological model in-
volving the retarded elastic response is more accurate. Thus, one can
expect that the rheological terms associated to parameters α and χ,
apart from the values assigned to the other rheological parameters,
contribute to a better performance of the Phan-Thien and Tanner rhe-
ological model.

Additionally, it is also clear that for the take up velocity of 1000
m/min the velocity profile obtained numerically in this work ap-
proaches substantially better the experimental results available for the
PET melt when this prediction is compared with similar calculations

Table 4. Relative percentile differences D_v and D_T between numerical and
experimental values, for both velocity and temperature axial profiles
as they are defined in the main text.

Take up Velocity m/min	Retarded Elastic Response		Instantaneous Elastic Response		Maxwell Model		Newtonian Model	
	D_v	D_T	D_v	D_T	D_v	D_T	D_v	D_T
3000	3.18	12.46	6.7	20.9	7.0	19.51	15.58	17.26
2000	3.51	17.31	5.52	26.12	5.45	26.62	2.23	21.95
1000	4.5	8.3	4.1	16.0	4.34	11.15	17.14	10.24

carried out previously in the literature for the same spinning conditions. In fact, for the one mode Phan-Thien and Tanner model with instantaneous elastic response, without the term $d \ln T/dt$ and with different rheological parameters ($\chi = 0$, $\xi = 0.015$ and $\lambda_{00} = 2.048 \ 10^{-3}$ s), Gagon and Denn [3] reported and discussed that numerical predictions are following a different trend from that of the experimental values obtained by George [6] at this take up velocity only. We reproduced consistently the numerical results reported by these authors and found that D_v is between 5 and 15%. Consequently, the improvement obtained with our model and calculations may be attributed mainly to the following aspects considered in the model: (a) evaluation of rheological parameters by fitting simultaneously both sets of experimental data: shear rate flow [16] and spinning flow [6] (see also the difference between elongational viscosities reported in Figure 3), (b) consideration of the rate of change of temperature in the rheological model, (c) consideration of the PET thermophysical properties as function of temperature, (d) inclusion of the heat dissipation term in the energy balance, (e) use of improved correlations for the air-filament heat transfer and friction coefficients which have been recently proposed by Denn [10], (f) inclusion of the internal heat transfer coefficient, and (g) consideration of the retarded elastic response, which allows us to impose the initial conditions at the maximum filament swelling.

It is important to mention here that the Maxwell rheological model ($\chi = 0$, $\xi = 0$ and $\lambda_{00} = 0.01425$ s) can predict the spinning experimental velocity relatively well. Thus, for this case D_v is between 4.34 and 7%. This aspect is very consistent with the fact that for the Phan-Thien and Tanner model, either with retarded and instantaneous elastic responses, the values of the rheological parameters χ and ξ are rather small, of the order of 10^{-5}. On the other hand, the Maxwell model can only predict the lower asymptote of the shear rate flow as it is shown in Figure 2.

In order to complete the above discussion, we carried out calculations with the Newtonian fluid, for $\beta = 0.44$ and $\psi = 0.26$ to get the best fit of experimental data. It is found that D_v is between 2.23 and 17.14% (see Table 4). Thus, significant increases of the percentile error are observed when the take up velocity is changed from 2000 m/min to any of the other values.

Before analyzing the numerical temperature profiles, from the above discussion the following conclusions can be formulated in relation to the prediction of the axial velocity profile: (a) in the spinning of the PET melt, a full non-linear rheological model should be considered, like the Phan-Thien and Tanner model with retarded elastic response
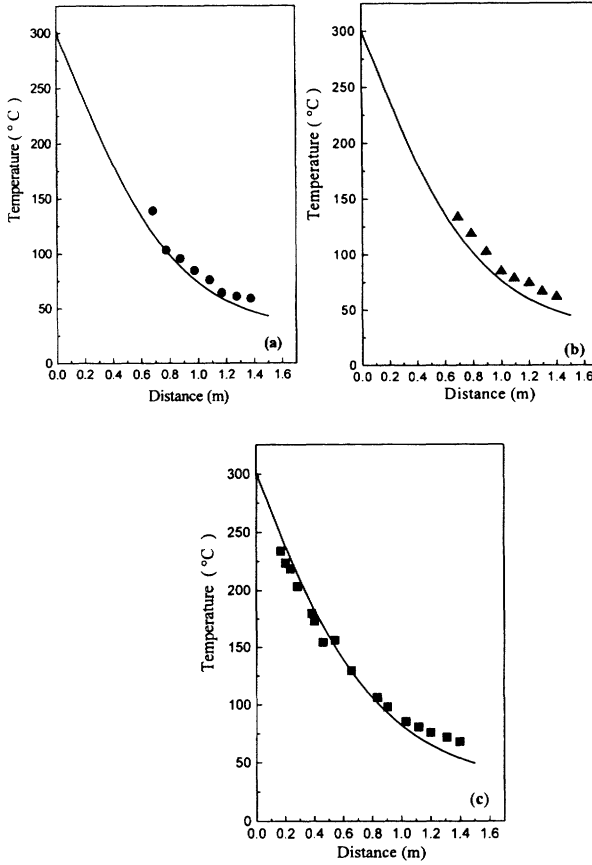
FIGURE 5. Numerical predictions (solid lines) of the filament temperature profile for the spinning conditions of Table 1 and by using the Phan-Thien and Tanner model with retarded elastic response ($\alpha = 0.8$, $\beta = 0.4$ and $\psi = 0.22$). Temperature experimental data [6] are indicated with symbols for the following take up velocities: (a) solid circles for 3000 m/min; (b) solid triangles for 2000 m/min, (c) solid squares for 1000 m/min.

as it is described by Equations (1) to (5), mainly in the case that the take up velocity is relatively small, and (b) the characterization (determination of the rheological parameters) of the non-linear rheological models should be carried out with the help of both shear and elongational flows.

Figures 5(a to c) show that numerical temperature profiles are in qualitative agreement with experimental values [6], when $\alpha = 0.8$ for the three take up velocities studied in this work (1000, 2000 and 3000 m/min). Additionally, with the help of Table 4, one may conclude once more that the Phan-Thien and Tanner model with retarded elastic response gives the best prediction in the framework of the spinning model proposed in this work when both values D_T and D_v are considered. It is also observed that the minimum error of D_T is obtained for the lower take up velocity studied [Figure 5(c)]. The rheological alternatives discussed in this work clearly indicate that the spinning model predicts the polymer temperature profile with less precision at larger distances from the extrusion capillary. This may be associated to the axial change of the polymer thermal conductivity, which is a consequence of the chain ordering caused by the stretching flow. In any case the numerical predictions shown in Figure 5 are improvements of those calculated with models already presented in the literature as it may be appreciated from Table 4.

CONCLUSIONS

A thermo-rheological model is formulated to describe quantitatively the PET melt spinning process at relatively low take up velocities. Theoretical results are compared with well documented experimental data of this process published previously. It is found that the Phan-Thien and Tanner model with retarded elastic response gives the best velocity and temperature predictions in the framework of the spinning model proposed, when it is compared with the predictions of other models already used in the literature. This improvement may be attributed additionally to several aspects considered in our work.

The rheological behavior of the PET melt with an intrinsic viscosity $[\eta]_0 = 0.675$ dl/g and an average molecular weight $Mw = 43,744$ Da can be effectively modeled with the Phan-Thien and Tanner model with retarded elastic response. Since the parameters that affect the non-linear terms of this rheological model are rather small, the PET melt has a viscoelastic response similar to that of the Maxwell fluid for spinning flows at relatively low take up velocities. This is not true for

shear flow at high shear rates where pseudoplastic behavior is observed. Thus, from the experience gained in the calculations carried out in this work, it is clear that for the appropriate characterization of a viscoelastic material with a non-linear rheological model, experimental data of shear and elongational flows at different temperatures are definitely required.

ACKNOWLEDGMENTS

REFERENCES

1. Fisher, R. J. and M. M. Denn. 1977. *AIChE J.,* 23:23–28.
2. Denn, M. M. 1983. *Computational Analysis of Polymer Processing,* Eds. J. R. A. Pearson and S. M. Richardson, 179–216, Applied Science Publishers, New York.
3. Gagon, D. K. and M. M. Denn. 1981. *Polym. Eng. Sci.,* 21:844–853.
4. Gupta, R. K. and A. B. Metzner. 1982. *J. Rheology,* 26:181–198.
5. Devereux, B. M. and M. M. Denn. 1994. *Ind. Eng. Chem. Res.,* 33:2384–2390.
6. George, H. H. 1982. *Polym. Eng. Sci.,* 22:292–299.
7. Dutta, A. 1987. *Polym. Eng. Sci.,* 27:1050–1058.
8. Henson, G. M., D. Cao, S. E. Bechtel and M. G. Forest. 1998. *J. Rheology,* 42:329–360.
9. Keunings, R., M. J. Crochet and M. M. Denn. 1983. *Ind. Eng. Chem. Fundam.,* 22:347–355.10.
10. Denn, M. M. 1996. *Ind. Eng. Chem. Res.,* 35:2842–2843.
11. Phan-Thien, N. and R. I. Tanner. 1977. *J. Non-Newt. Fluid Mech.,* 2:353–346.
12. Phan-Thien, N. 1978. *J. Rheology,* 22:259–283.
13. Phan-Thien, N. 1979. *J. Rheology,* 23:451–456.
14. Sugeng, F., N. Phan-Thien and R. Y. Tanner. 1987. *J. Rheology,* 31:37–58.
15. Denn, M. M. 1990. *Ann. Rev. Fluid Mech.,* 22:13–34.
16. Gregory, D. R. and M. T. Watson. 1970. *J. Polym. Sci.,* 30:399–406.
17. Joseph, D. D., M. Renardy and J. C. Saut. 1985. *Arch. Ration. Mech. Anal.,* 87:213–251.

18. Hatzikiriakos, S. G., G. Heffner, D. Vlassopoulos and K. Christodoulou. 1997. *Rheol. Acta,* 36:568–578.

19. Denn, M. M. 1980. *Ann. Rev. Fluid Mech.,* 12:365–387.

20. Ziabicki, A. and H. Kawai. 1985. *High-Speed Fiber Spinning.* Wiley, New York.

21. Papanastasiou, T. C., V. D. Dimitriadis, L. E. Scriven, C. W. Macosko and R. L. Sani. 1996. *Adv. Polym. Tech.,* 15:237–244.

22. Petrie, C. J. S. 1978. *J. Non-Newt. Fluid Mech.,* 4:137–145.

23. Petrie, C. J. S. 1979. *Elongational Flows.* Pitman, London.